Gigapixel-like imaging strategies for dental anthropology: Applications for scientific communication and training in digital image analysis

John C. Willman[a, b, c*]
Marina Lozano[b, c]
Raquel Hernando[c, b]
Josep Maria Vergès[b, c]

[a] Laboratory of Prehistory, CIAS – Research Centre for Anthropology and Health, Department of Life Sciences, University of Coimbra, 3000-456 Coimbra, Portugal

[b] IPHES, Institut Català de Paleoecologia Humana i Evolució Social, 43007 Tarragona, Spain

[c] Àrea de Prehistòria, Universitat Rovira i Virgili (URV), 43002 Tarragona, Spain

*Communicating author: john.willman@uc.pt

Key words: scanning electron microscopy, photomosaic, extended focus, El Mirador Cave, dental wear, cingular continuous lesion

Abstract

Gigapixel and gigapixel-like (GPL) imaging strategies are a powerful means of communicating scientific results of visual observations in academic and public spheres. GPL images are made from a photomosaic of multiple, adjacent extended focus images, which allows users to "pan and zoom" across a surface to document or analyze specific features. Microscopic approaches using GPL imaging strategies are gaining popularity in use-wear analyses of lithics and bone implements but have not been applied to the study of human skeletal or dental remains. Here we present three examples of GPL imaging using scanning electron microscopy (SEM) of the dental surfaces of teeth excavated from the Chalcolithic contexts of El Mirador Cave (Sierra de Atapuerca, Burgos, Spain). Numerous common features are identifiable in the GPL examples from El Mirador Cave that include wear features (e.g., enamel chipping, labial striations), perikymata, calculus deposits, hypoplasias, and postmortem taphonomic features. One GPL example shows a less-commonly documented pair of lingual surface features (i.e., lingual surface attrition of the maxillary anterior teeth [LSAMAT] and a continuous cingular lesion [CCL]) for which co-occurrence has not been previously documented. Another example using a combination of GPL, macrophotography, and additional high magnification SEM images shows a clear case of chemical erosion on a labial surface of the tooth - a seldom documented form of wear in bioarchaeological contexts. This latter example also highlights the complementary nature of SEM (and GPL) with digital macrophotography for documenting dental wear features. Together, these examples illustrate the utility of GPL images of dental surfaces for didactic purposes and analysis.

Introduction

Dental anthropology makes considerable use of microscopic observations and analyses that include dental microwear analyses of dietary and non-dietary tooth-using behaviors (Teaford et al., 2001; Semprebon et al., 2004; Teaford, 2007; Ungar et al., 2008; Lozano et al., 2008, 2017; Romero and De Juan, 2012; Krueger, 2016; Willman, 2016, 2017; Hernando et al., 2020), anomalous features (Bondioli et al., 2012; Dori and Moggi-Cecchi, 2014); incremental growth (Guatelli-Steinberg et al., 2007; Hillson, 2014; Modesto-Mata et al., 2017), stress indicators and growth disruption (Guatelli-Steinberg et al., 2004, 2013; Hillson, 2014; McGrath et al., 2018), calculus inclusions (Power et al., 2015; Sperduti et al., 2018; Bucchi et al., 2019), and taphonomy (King et al., 1999; Martínez and Pérez-Pérez, 2004) among many other topics. An historical emphasis and continued use of optical light microscopy and scanning electron microscopy (SEM) in dental anthropology has expanded to include other microscopic imaging technologies such as white light confocal microscopy (Teaford, 2007; Ungar et al., 2008; Schmidt et al., 2019; Ungar, 2019) and 3D microscopy (Hillson et al., 2010; Bello, 2011). However, optical light microscopy (*sensu lato*) and SEM are still powerful tools for the rapid data collection for some dental features, and the visualization of others, in addition to being more widely available to researchers compared to some forms of microscopy (e.g., confocal and Focus Variation Microscope allowing 3D reconstruction). However, there are some shortcomings associated with optical light microscopy and SEM in dental anthropology. For instance, two-dimensional images of three-dimensional surfaces can leave some aspects of an image out of focus or distorted – an issue that was particularly prevalent in the transition from SEM-based microwear analyses to the use of confocal microscopy and scale-sensitive fractal analysis for dental microwear texture analysis (Ungar et al., 2008; Hernando et al., this issue). Another issue occurs when features of interest (e.g., instrumental striations or perikymata along an entire labial/buccal surface) can be larger than the entire field of view when using high magnification. These issues and others mean that researchers often negotiate between magnification, depth of field, and field of view. Stitching adjacent images into mosaic or composite images is a common way of dealing with issues of magnification versus field of view (e.g., Ryan and Johanson, 1989; Egocheaga et al., 2004; Guatelli-Steinberg and Reid, 2010; Hillson et al., 2010; Willoughby et al., 2018), and the use of focus-stacking to create extended focus images can deal with depth of field issues (e.g., Willman et al., 2019). However, changing microscope settings during the acquisition of a series of images to be stitched often contributes to final mosaics with less than seamless blending. Furthermore, depth of field is generally not reasonably dealt with when subjects in an image are not flat, leaving aspects of mosaics out of focus and further contributing to poorly blended composite images.

With these issues in mind, we describe a microscopic approach that uses focus-stacking (extended focus images) and panoramic stitching to create mosaic images with high depth of field using SEM. This "gigapixel-like" (GPL) imaging strategy (Vergès and Morales, 2014) can be used to create multiscale, high-resolution images of entire dental surfaces that can be viewed from a field of view that encompasses an entire surface to high magnification views of dental microstructure, microwear, taphonomic features, among other features. The strict definition of gigapixel images states that they are bitmap images containing at least one billion pixels, but many are simply large mosaics of high-resolution digital photographs (Vergès and Morales, 2014). The term "gigapixel-like" is used to denote that the gigapixel concept is employed, but a smaller number of pixels are generally used in contrast to traditional gigapixel images. Gigapixel and GPL images are not only useful for analysis, but also for scientific communication, publication, and training researchers (Louw and Crowley, 2013; Vergès and Morales, 2014). Gigapixel and GPL images are highly interactive, social, and participatory – characteristics that are ideal for teaching and communicating scientific results with the public (Louw and Crowley, 2013). Web-based viewers are available to publish GPL images online (Louw and Crowley, 2013; Vergès and Morales, 2014), and the original images can be included as data supplements to research articles to allow other researchers to reconstruct GPL images or independently verify results (Vergès and Morales, 2014).

The utility of gigapixel and GPL strategies for imaging petroglyphs (Louw and Crowley, 2013), shale microstructure (Fauchille et al., 2018), entomological specimens (Holovachov et al., 2014), and other subjects has been explored. Archaeological applications of GPL strategies have explored lithic use-wear with SEM (Vergès and Morales, 2014) and reflected light microscopy for lithic use-wear (Fernández-Marchena et al., 2016) and retouch modifications from bone instruments (Mateo-Lomba et al., 2019). The present study concentrates on examples of macro- to microscopic features on dental tissues using SEM as a means of creating multi-scale mosaic images for didactic purposes ranging from scientific publication to teaching and outreach. Through improved teaching and communication of scientific results, GPL imaging strategies can help reduce inter- and intraobserver identification error, provide a cost-effective means for initial observational training before transitioning to data acquisition with a microscope, and improve scientific communication in professional and public spheres.

Materials and Methods

Examples for the present study are derived from the site of El Mirador Cave (Ibeas de Juarros, Burgos), on the southern slope of the Sierra de Atapuerca, where systematic excavations are ongoing since the 1999 (Vergès et al., 2002, 2008, 2016). The human remains studied here come from Chalcolithic burial context dating between 4000 ± 30 BP (4550-4390 cal. BP) and 4120 ± 30 BP (4880-4480 cal. BP) (Vergès et al., 2016). The dentitions from the site were the subject of previous analyses of non-alimentary uses of the anterior dentition (Lozano et al., 2017), buccal and occlusal microwear of the deciduous teeth of children (Hernando et al. 2020), morphological trait variation and pathology (Ceperuelo et al., 2015), root canal morphology (Ceperuelo et al., 2014), incremental growth analyses (Modesto-Mata et al., 2017), and microfossils in dental calculus (Bucchi et al., 2019).

Three anterior teeth were chosen for GPL image construction using two different surfaces: the labial surface of a left mandibular lateral incisor (I_2), the lingual surface of a right maxillary central incisor (I^1), and the labial surface of another right I^1. One of us (JCW) is currently analyzing variation in anterior dental wear features for the El Mirador collection, and chose the three examples used here on the basis of observations made macroscopically and with low magnification (~3x headset magnifier with LED light source). The intent was to choose teeth with a variety of wear and morphological features that could be used for didactic purposes. In particular, the examples explore GPL construction with teeth of different size (I^1 and I_2), and the complexity of the surface (smooth labial versus rugose lingual). Enamel surfaces were gently cleaned with alcohol and cotton applicators prior to visualization using an environmental scanning electron microscope (ESEM: FEI Quanta 600) in low vacuum mode.

SEM working distance was variable throughout analyses to collect image stacks for the creation of extended focus images. Working distance was between 10-20 mm for the entirety of each image acquisition period. All other SEM parameters (brightness, contrast, stage tilt, etc.) were held constant during image acquisition (Vergès and Morales, 2014). Each tooth surface was oriented as close to horizontal with respect to the detector as possible to reduce the number of images needed for each extended focus image set. Accelerating voltage was set at 20 kV.

The number of micrographs taken at each position on the tooth varies based on the local depth of field. For example, in labial view, the mesial and distal edges of the tooth and root have greater depth of field than the center of the labial surface, which requires more images (e.g., about five to eight) in the former compared to the latter cases (e.g., about two to four). As working distance is adjusted to achieve a focus stack set for an extended focus image, it is better to take too many images than too few. Those images that are too out of focus to be included in an extended focus image stack can be removed later (see **Supplemental Data**). After completing an image set at one location, move to an adjacent area on the same tooth taking care to overlap with the previous focus stack by ~20-25% to ensure adequate photomerging later in the process (Vergès and Morales, 2014).

The creation of extended focus images from a stack of images can be accomplished using a variety of free software options such as Hugin (http://hugin.sourceforge.net/) and ImageJ (https://imagej.nih.gov/ij/), or other subscription-based services like Adobe Photoshop CS6 or Helicon Focus (Helicon Soft Ltd.). Likewise, the same software packages and others (e.g., Microsoft Image Composite Editor [also freely available]: https://www.microsoft.com/en-us/research/product/computational-photography-applications/image-composite-editor/) can be used to stitch and merge the extended focus images into a photomosaic. The present analysis uses Photoshop CS6 and Microsoft ICE for the creation of GPL images. Guidelines outlining the full process for creating a GPL image is explained in a tutorial in the open access **Supplemental Data**.

Results

Example 1 – Labial surface of a left I_2

The labial incisor surface of ATA09-MIR201-REM-489, a left I_2, provides a number features to be explored with GPL panning and zooming (**Figure 1**). A series of enamel chips of small to medium size (grades 1 and 2: Bonfiglioli et al., 2004) present well-worn edges indicating an antemortem origin (Scott and Winn, 2011). Microstriations are also visible across the labio-occlusal edge and labial surface, as well as right-oblique instrumental striations that suggest the individual performed certain non-alimentary behaviors with the right hand (Bermúdez de Castro et al., 1988). Some perikymata can be seen in addition to a furrow-form hypoplasia. A small deposit of calculus (grade 1: Brothwell, 1981) is present in the cervical third of the labial surface. Subtle postdepositional cracking of the root surface is also easily visualized. While not an exhaustive list of features present on the surface, these few examples show the utility of panning and zooming with a GPL image for the visualization of microscopic features on dental surfaces.

Example 2 – Lingual surface of a right I^1

The lingual surface of ATA12-MIR201-S36-69, a right I^1 (**Figure 2**), is particularly interesting with respect to behavioral reconstruction. The tooth exhibits lingual surface attrition of the maxillary anterior teeth (LSAMAT: Turner and Machado, 1983) involving the enamel and exposing dentin in the cervical third of the lingual surface (grade 2: Tanga et al., 2016). A faint continuous cingular lesion (CCL: Dori and Moggi-Cecchi, 2014; Carrasco et al., 2017; Marado et al., 2017) is also present. While the exact aetiology of CCL is poorly understood, the lesions are probably due to erosion (Dori and Moggi-Cecchi, 2014; Carrasco et al., 2017), although some hypothesize that they are related to abrasive wear from non-alimentary behaviors like fiber or cordage processing (Marado et al., 2017). The lack of localized striations on the CCL suggests an erosive origin in this case. However, the co-occurrence of CCL and LSAMAT has not been previously documented and may indicate that both abrasive and erosive behaviors are contributing to this unique combination of wear features. Multiple antemortem enamel chips are present (grades 1 and 2). Postdepositional cracking and splitting of enamel and dentin is also visible.

Example 3 – Labial surface of a right I^1

The labial surface of ATA-MIR201-S36-68, a right I^1 (**Figure 3**), also exhibits features of interest for behavioral reconstruction. The color macrophotograph shows appreciably darker enamel in the middle third of the crown compared to areas immediately surrounding it. The darker color and localized dullness of enamel indicates some thinning of the overlying enamel. These characteristics are commonly associated with erosive wear in clinical studies (Johansson et al., 1996, 2012; Ganss et al., 2014), but erosion is rarely documented in archaeological materials (reviewed in: Coupal and Sołtysiak, 2017). A GPL image was made to transect the lesion to further explore the microscopic wear patterning (**Figure 3**).

The cervical-most portion of the GPL image shows a lack of striations, well-preserved enamel lacking striations, and a calculus deposit. Just below the calculus deposit, moving toward the incisal surface, there is a heavy concentration of striations with predominately horizontal to slight right-oblique orientation. The cervical-most striations (immediately incisal to the calculus deposit) are less well-defined (shallower, narrower) than those closer to the incisal edge which are wide with greater rounding of their borders. The cervical to incisal patterning of striations corresponds closely to the color/luster gradient seen in the macrophotograph – the areas of "bright" and well-preserved enamel have more well-defined striations whereas the striations overlying the darkest/dullest enamel are poorly defined. A micrograph (not used for the construction of the GPL image of this tooth) was taken at higher magnification (300x) to obtain details of suspected erosion (**Figure 4**).

The higher magnification detail (**Figure 4**) of the dark and dull enamel surface shows the characteristic "honeycomb" pattern of prism exposure caused by chemical erosion. Coupal and Sołtysiak (2017) suggest using magnification of 300x to observe chemically eroded surfaces. However, we note here that it is more important to include a scale bar or an indication of the horizontal field of view in a micrograph than relying on magnification alone (Borel et al., 2014; Martín-Viveros and Ollé, 2020; Hernando et al., this issue). Nevertheless, erosion and instrumental striations are evident on the middle third of the labial face (**Figure 4**).

The complementary use of SEM and optical light microscopy for studying use-wear and residues on stone tools is well-established (e.g., Borel et al., 2014; Ollé et al, 2016; Pedergnana and Ollé, 2018), and the use of optical light microscopy as an alternative to SEM for the analysis of buccal dental microwear is promising (Hernando et al., this issue). Combinations of optical and SEM observations are sometimes used to examine, describe, and visually document various dental wear features on hominin teeth (e.g., Lozano et al., 2013; Xing et al., 2017; Willman et al., 2019). These dental-based studies generally use some form of optical light microscopy (*sensu lato*), at lower low magnification (less than 200x), in combination with SEM-based observations ranging from low to high magnification as a means of improving interpretation and visualization of various dental wear features. The combination of digital macrophotography and SEM in the present study (**Figure 3**) also shows how the use of more than one visualization methodology can enhance descriptive and visual presentation of dental wear features (see also Willman, 2016; Willman et al., 2020). While digital (macro)photography is a commonly available resource for studying fossil and subfossil human teeth, portable or tabletop optical light microscopy (*sensu lato*) may not be. The ATA-MIR201-S36-68 tooth was chosen for GPL imaging in part because of the curious enamel color (dark) and luster (dull) of the labial surface. Had the tooth simply been molded with silicone and observed as a translucent or opaque dental cast at a later date (as is common in many fossil-oriented SEM studies), the eroded surface may not have been as easily identified as interesting enough to observe at higher magnification using SEM. Therefore, we suggest that digital documentation of the original dental surfaces – either with (macro)photography or other low-magnification approaches (e.g., forms of optical light microscopy, *sensu lato*) – should be included alongside the micrographs obtained using SEM when possible in bioarchaeological and paleoanthropological investigations of human dental wear features.

As with the example of ATA09-MIR201-REM-489, the orientation of the striations probably indicates a right-handed manipulative behavior producing the striations (Bermúdez de Castro et al., 1988). The predominately horizontal orientation of the striations is similar to the pattern observed in the Mesolithic human teeth from El Collado (Oliva, Valencia, Spain) and a Neolithic individual from St. Pau (Barcelona, Spain: Lalueza-Fox, 1992). The absence of striations above the large calculus deposit, the presence of fine striations just below the calculus deposit, and the presence of wider striations with well-worn margins closer to the incisal edge is interesting. Macroscopic enamel chipping is also apparent on the incisal edge.

A repetitive manipulative behavior that avoided contact between the exogenous, manipulated material and the gingiva may explain the cervical to incisal distribution of labial surface striations and incisal chipping. However, the labial erosion is somewhat unique in the present study, given how few studies document dental erosion in archaeological contexts (Robb et al., 1991; Kieser et al., 2001; Ganss et al., 2002; Lanigan and Bartlett, 2013; Tomczyk and Zalewska, 2016; Coupal and Sołtysiak, 2017). At this point, it is unclear from a single example whether the chemical erosion, striations, and dental chipping resulted from a singular behavior or multiple distinct behaviors. However, the etiology and prevalence of dental erosion in the El Mirador sample is beyond the scope of the present paper, and we cannot extrapolate our results for three dental surfaces to the entire dental sample. As previously noted, a complete analysis of El Mirador anterior dental wear is currently underway.

Discussion and Conclusion

The multi-scale mosaic images of dental surfaces created here illustrate the broad applications of GPL imaging strategies for didactic purposes ranging from scientific publication, to teaching and outreach. The analysis of dental wear features, incremental growth, calculus deposits, pathology, enamel erosion, and other visually identified features commonly studied by dental anthropologists are well-suited to study and visualization using GPL imaging strategies. Furthermore, technicians can create the raw images necessary for the creation of GPL images that can then be studied and analyzed by trained observers after the acquisition process (Louw and Crowley, 2013; Louw et al., 2013; Vergès and Morales, 2014).

Museums are increasingly integrating digital content into exhibits and websites for public communication of scientific media as well as art and cultural media. The proliferation of software to create Gigapixel and GPL images, has been accompanied by online hosts for sharing and annotating them (www.gigamacro.com, www.gigapan.com). The ability to "pan and zoom" with GPL images offers another way in which the public can interact with scientific content in a self-guided manner (Louw and Crowley, 2013; Louw et al., 2013). Trained researchers can identify features of interest through annotation to create "scavenger hunts" for training purposes and public interaction with GPL images. Thus, the use of GPL imaging in dental anthropology has far reaching possibilities for teaching and communication of scientific results, reducing inter- and intraobserver identification error, providing a cost-effective means for training researchers in microscopic observational protocols, and improving scientific communication in professional and public spheres.

We intentionally focused on the use of GPL images in the present work for qualitative analyses, training, and outreach rather quantitative analyses. This is partially because several factors may introduce measurement "noise" or mask specific features in the extended focus image and the process of creating a mosaic GPL image (also see: **Supplemental Data**). Some factors include, but are not limited to: differences in working distance and/or number of images used in each extended focus image stack that make up a single GPL mosaic, total surface depth or surface heterogeneity of an object being analyzed, the magnification under which observations are made, and the software – and methods within each software program – used to stack and stitch images. We have addressed some of these issues here (see **Supplemental Data**), but it should be noted that the methodology outlined here is provided as a guideline for producing the most appropriate GPL images for the desired research, training, or outreach purposes. For example, the initial examples (**Figure 1** and **2**) of whole surfaces are more likely to create distortion or mask features (especially along the edges of highly curved aspects of the tooth) compared to the relatively simple, flat GPL featured in the final example (**Figure 3**). The final image (**Figure 3**), is unlikely to exhibit distortion of measurements given the parameters of the software (Microsoft ICE) used to create the final GPL (see also Fernández-Marchena et al., 2016 for an similar example featuring rock crystal). In contrast, the complex shape of entire tooth surface (**Figure 1** and **2**), or similar objects, may necessitate less stringent algorithms for the stitching of mosaics that impart some imperfections or distortions in a final GPL image (see **Supplemental Data**). The researcher must make these decisions and the accuracy of the images should be described in the text or supplemental data, or more reasonably – the raw data (original micrographs/images) should be made open access so other researchers can independently assess their reliability for their purposes.

GPL will not replace the need to re-analyze dental fossil surfaces completely – especially since it represents only one form of visual documentation of a surface. While, many researchers already rely on casts to prevent unnecessary handling of original specimens (see also: Hernando et al, this issue), high-resolution GPL images of original fossils may further reduce the need for some re-analysis and handling. Furthermore, GPL images may also enhance remote collaboration between research institutions and curators while simultaneously creating materials to enhance public engagement with this form of scientific communication. Another area of potential elaboration of the GPL approach may be SEM-based microphotogrammetry (e.g., Ball et al., 2017). While this approach would require an even greater amount of uninterrupted SEM use for image acquisition, the creation of 3D models may provide an answer to some issues associated with poor image stitching, loss of resolution, or masking of features along the edges of objects with high relief we encountered with the dental examples here.

Lastly, it is not known whether the dental wear features documented here using GPL imaging strategies are representative of the entire dental sample from El Mirador Cave, but CCL and labial erosion are seldom documented in bioarchaeological analyses of dental wear. Nevertheless, these three examples illustrate the multifactorial nature of dental wear while simultaneously illustrating the utility of GPL imaging strategies to document disparate features on dental surfaces. We also make an argument that SEM (and SEM-based GPL reconstructions) can be complimented by using optical light microscopy and/or digital (macro)photography of the original dental surfaces – a practice that is exceedingly common in microscope-based studies of archaeological material culture but less commonly employed for the analysis of human remains. We are just beginning to understand the broader geographic and temporal distributions of non-alimentary behaviors in the Holocene. GPL images offer one means of thoroughly documenting unique forms of wear. GPL images can be downloaded and used to train other researchers in observation protocols; thus, continuing to expand the current spatiotemporal distribution and improve interpretations of these traces of past human behaviors written on the surfaces of teeth.

Acknowledgements

We thank the Scientific and Technical Resource Service of Rovira i Virgili University in Tarragona provided access and assistance to the ESEM. This research is supported by funding from the Marie Skłodowska-Curie Actions (H2020-MSCA-IF-2016 No. 749188 and H2020-MSCA-IF-2018 No. 839822), AGAUR (Ref. 2017SGR1040) and URV (Ref. 2017PFR-URV-B2-91) Projects, MICINN/FEDER (Ref. PGC2018-093925-B-C32), and URV Martí-Franquès Research Grant (URV-2019PMF-PIPF-59).

Supplementary Data

The micrographs used in the construction of GPL images used in this manuscript, as well as the extended focus images, final GPL images, and detailed instructions for creating GPL images are available open access at (ZENODO.org link will be provided in final version approved for publication).

References

Ball, A.D., Job, P.A., Walker, A.E., 2017. SEM-microphotogrammetry, a new take on an old method for generating high-resolution 3D models from SEM images. J. Microscopy. 267 (2) , 214-226.

Bello, S.M., 2011. New results from the examination of cut-marks using three-dimensional imaging. In: Ashton, N.M., Lewis, S.G., Stringer, C.B., (Eds.), The Ancient Human Occupation of Britain. Amsterdam: Elsevier, pp. 249-262.

Bermúdez de Castro, J.M., Bromage, T.G., Jalvo, Y.F., 1988. Buccal striations on fossil human anterior teeth: evidence of handedness in the middle and early Upper Pleistocene. J. Hum. Evol. 17 (4), 403-412. https://doi.org/10.1016/0047-2484(88)90029-2.

Bondioli, L., Coppa, A., Frayer, D.W., Tartaglia, G., Vidale, M., Macchiarelli, R., 2012. Dental lesions on the permanent teeth at Neolithic Mehrgarh, Pakistan. In: Lefèvre, V., (Ed.), Orientalismes De l'Archaéologie au Musée Mélanges en l'honneur de Jean-François Jarrige. Turnhout: Brepols Publisher, pp. 115-126.

Bonfiglioli, B., Mariotti, V., Facchini, F., Belcastro, M.G., Condemi, S., 2004. Masticatory and non-masticatory dental modifications in the Epipalaeolithic necropolis of Taforalt (Morocco). Int. J Osteoarchaeol. 14 (6), 448-456. doi:10.1002/oa.726.

Borel, A., Ollé, A., Vergès, J.M., Sala R., 2014. Scanning Electron and Optical Light Microscopy: two complementary approaches for the understanding and interpretation of usewear and residues on stone tools. J. Archaeol. Sci 48, 46-59. https://doi.org/10.1016/j.quaint.2016.02.005.

Brothwell, D.R., 1981. Digging Up Bones: The Excavation, Treatment, and Study of Human Skeletal Remains. Ithaca: Cornell University Press.

Bucchi, A., Burguet-Coca, A., Expósito, I., Aceituno Bocanera, F.J., Lozano, M., 2019. Comparisons between methods for analyzing dental calculus samples from El Mirador cave (Sierra de Atapuerca, Spain). Archaeol. Anthropol. Sci. 11 (11), 6305-6314. doi: 10.1007/s12520-019-00919-z.

Carrasco, S.R., Bonilla, M.D.-Z., Mateo, V.F., Sanjuán, L.G., 2017. Bioarchaeological analysis at the Copper Age site of Valencina de la Concepción (Seville, Spain): The PP4-Montelirio sector. In: Tomé, T., Bonilla, M.D.-Z., Silva, A.M., Cunha, C., Boaventura, R., (Eds.), Current Approaches to Collective Burials in the Late European Prehistory. Oxford: Archaeopress, pp. 103-118.

Ceperuelo, D., Lozano, M., Duran-Sindreu, F., Mercadé, M., 2015. Supernumerary fourth molar and dental pathologies in a Chalcolithic individual from the El Mirador Cave site (Sierra de Atapuerca, Burgos, Spain). Homo. 66 (1), 15-26. doi:https://doi.org/10.1016/j.jchb.2014.05.007.

Ceperuelo, D., Lozano, M., Duran-Sindreu, F., Mercadé, M., 2014. Root Canal Morphology of Chalcolithic and Early Bronze Age Human Populations of E l M irador C ave (S ierra de A tapuerca, S pain). Anatom. Rec. 297 (12), 2342-2348. doi:10.1002/ar.22958.

Coupal, I., Sołtysiak, A., 2017. Dental erosion in archaeological human remains: A critical review of literature and proposal of a differential diagnosis protocol. Arch. Oral Biol. 84 (Supplement C), 50-57. https://doi.org/10.1016/j.archoralbio.2017.09.011.

Dori, I., Moggi-Cecchi, J., 2014. Brief Communication: An enigmatic enamel alteration on the anterior maxillary teeth in a prehistoric North Italian population. Am. J. Phys. Anthropol. 154 (4), 609-614. doi:10.1002/ajpa.22535.

Egocheaga, J.E., Pérez-Pérez, A., Rodríguez, L., Galbana, J., Martínez, L.M., Antunes, M.T., 2004. New evidence and interpretation of subvertical grooves in Neandertal teeth from Cueva de Sidron (Spain) and Figueira Brava (Portugal). Anthropol. 42, 49-52. https://www.jstor.org/stable/26292671.

Fauchille, A., Van den Eijnden, A., Ma, L., Chandler, M., Taylor, K., Madi, K., Lee, P., Rutter, E., 2018. Variability in spatial distribution of mineral phases in the Lower Bowland Shale, UK, from the mm-to µm-scale: Quantitative characterization and modelling. Mar. Petrol. Geol. 92, 109-127. https://doi.org/10.1016/j.marpetgeo.2018.02.029.

Fernández-Marchena, J.L., Ollé, A., Rodríguez-Nóvoa, A.A., Amado-Rodríguez, E., Díaz-Rodríguez, M., Pérez-Tenorio, R., de la Torre-Llorca, M.J., 2016. Traceological analysis of a singular artefact: The rock crystal point from O Achadizo (Boiro, A Coruña, Galicia). J. Lithic Stud. 3 (2), 1-19. doi:10.2218/jls.v3i2.1542.

Ganss, C., Klimek, J., Borkowski, N., 2002. Characteristics of tooth wear in relation to different nutritional patterns including contemporary and medieval subjects. Euro. J. Oral Sci. 110 (1), 54-60. https://doi.org/10.1034/j.1600-0722.2002.00117.x.

Ganss, C., Lussi, A., 2014. Diagnosis of erosive tooth wear. In: Lussi A, and Ganss C, (Eds.), Erosive Tooth Wear: A Phenomenon of Cultural Significance. Basel: Karger Publishers, pp. 22-31.

Guatelli-Steinberg, D., Buzhilova, A.P., Trinkaus, E., 2013. Developmental stress and survival among the Mid Upper Paleolithic Sunghir children: Dental enamel hypoplasias of Sunghir 2 and 3. Int. J. Osteoarchaeol. 23, 421-431. doi:10.1002/oa.1263.

Guatelli-Steinberg, D., Larsen, C.S., Hutchinson, D.L., 2004. Prevalence and the duration of linear enamel hypoplasia: a comparative study of Neandertals and Inuit foragers. J. Hum. Evol. 47 (1-2), 65-84. doi:10.1002/ajpa.10324.

Guatelli-Steinberg, D., Reid, D.J., 2010. Brief communication: The distribution of perikymata on Qafzeh anterior teeth. Am. J. Phys. Anthropol. 141 (1), 152-157. doi:10.1002/ajpa.21158.

Guatelli-Steinberg, D., Reid, D.J., Bishop, T.A., 2007. Did the lateral enamel of Neandertal anterior teeth grow differently from that of modern humans? J. Hum. Evol. 52 (1), 72-84.

Hernando, R., Willman, J.C., Vergès, J.M., Vaquero, M., Alonso, S., Oms, X., Cebrià, A., Morales, J.I., Lozano, M., 2020. Inferring childhood dietary maturation using buccal and occlusal deciduous molar microwear: A case study from the recent prehistory of the Iberian Peninsula. Archaeol. Anthropol. Sci. 12 (1), 30. doi:10.1007/s12520-019-00997-z.

Hernando, R., Fernández-Marchena, J.L., Willman, J.C., Ollé, A., Vergès, J.M., Lozano, M., this issue. Exploring the utility of optical light microscopy versus scanning electron microscopy for the quantification of dental microwear. Quat. Int.

Hillson, S., 2014. Tooth Development in Human Evolution and Bioarchaeology. Cambridge: Cambridge University Press.

Hillson, S.W., Parfitt, S.A., Bello, S.M., Roberts, M.B., Stringer, C.B., 2010. Two hominin incisor teeth from the middle Pleistocene site of Boxgrove, Sussex, England. J. Hum. Evol. 59:493-503. doi:10.1016/j.jhevol.2010.06.004.

Holovachov, O., Zatushevsky, A., Shydlovsky, I., 2014. Whole-drawer imaging of entomological collections: benefits, limitations and alternative applications. J. Conserv. Mus. Stud. 12 (1). http://doi.org/10.5334/jcms.1021218.

Johansson, A.-K., Johansson, A., Birkhed, D., Omar, R., Baghdadi, S., Carlsson, G.E., 1996. Dental erosion, soft-drink intake, and oral health in young Saudi men, and the development of a system for assessing erosive anterior tooth wear. Acta Odontol. Scand. 54 (6), 369-378. http://dx.doi.org/10.3109/00016359609003554.

Johansson, A,-K,, Omar, R,, Carlsson, G,E,, Johansson, A., 2012. Dental erosion and its growing importance in clinical practice: from past to present. Int. J. Dent. 2012. doi:10.1155/2012/632907.

Kieser, J.A., Dennison, K.J., Kaidonis, J.A., Huang, D., Herbison, P.G.P., Tayles, N.G., 2001. Patterns of dental wear in the early Maori dentition. Int. J. Osteoarchaeol. 11 (3), 206-217. https://doi.org/10.1002/oa.534.

King, T., Andrews, P., Boz, B., 1999. Effect of taphonomic processes on dental microwear. Am. J. Phys. Anthropol. 108 (3), 359-373. http://dx.doi.org/10.1002/(SICI)1096-8644(199903)108:3<359::AID-AJPA10>3.0.CO;2-9.

Krueger, K.L., 2016. Dentition, behavior, and diet determination. In: Irish J.D., Scott, G.R., (Eds.), A Companion to Dental Anthropology. Malden: John Wiley & Sons, Inc., pp. 396-411.

Lalueza-Fox, C., 1992. Information obtained from the microscopic examination of cultural striations in human dentition. Int. J. Osteoarchaeol. 2 (2), 155-169. https://doi.org/10.1002/oa.1390020207.

Lanigan, L., Bartlett, D., 2013. Tooth wear with an erosive component in a Mediaeval Iceland population. Arch. Oral Biol. 58 (10), 1450-1456. https://doi.org/10.1016/j.archoralbio.2013.06.019.

Louw, M., Ansari, A., Bartley, C., Sanford, C., 2013. Stories in the rock: a design case of an explorable image viewer in a natural history museum. Int. J. Des. Learn. 4 (2), 56-71.

Louw, M., Crowley, K., 2013. New Ways of Looking and Learning in Natural History Museums: The Use of Gigapixel Imaging to Bring Science and Publics Together. Curat. Mus. J. 56 (1), 87-104. doi:10.1111/cura.12009.

Lozano, M., Bermúdez de Castro, J.M., Arsuaga, J.L., Carbonell, E., 2017. Diachronic analysis of cultural dental wear at the Atapuerca sites (Spain). Quat. Int. 433, Part A, 243-250. http://dx.doi.org/10.1016/j.quaint.2015.08.028.

Lozano, M., Bermúdez de Castro, J.M., Carbonell, E., Arsuaga, J.L., 2008. Non-masticatory uses of anterior teeth of Sima de los Huesos individuals (Sierra de Atapuerca, Spain). J. Hum. Evol. 55 (4), 713-728. https://doi.org/10.1016/j.jhevol.2008.04.007

Lozano, M., Subirà, M.E., Aparicio, J., Lorenzo, C., Gómez-Merino, G., 2013. Toothpicking and periodontal disease in a Neanderthal specimen from Cova Foradà site (Valencia, Spain). PLoS ONE 8 (10), e76852. https://doi.org/10.1371/journal.pone.0076852

Marado, L.M., Cunha, C., Scott, G.R., Tomé, T., Machado, H., Silva, A.M., 2017. On the applicability of the assessment of dental tooth wear for the study of collective prehistoric burials. In: Tomé T, Bonilla MD-Z, Silva AM, Cunha C, and Boaventura R, (Eds.), Current Approaches to Collective Burials in the Late European Prehistory. Oxford: Archaeopress Archaeology, pp. 11-19.

Martín-Viveros, J.I., Ollé, A., 2020. Use-wear and residue mapping on experimental chert tools. A multi-scalar approach combining digital 3D, optical, and scanning electron microscopy. J. Archaeol. Sci. Rep. 30, 102236. https://doi.org/10.1016/j.jasrep.2020.102236.

Martínez, L.M., Pérez-Pérez, A., 2004. Post-mortem wear as indicator of taphonomic processes affecting enamel surfaces of hominin teeth from Laetoli and Olduvai (Tanzania): Implications to dietary interpretations. Anthropol. 42 (1), 37-42. http://www.jstor.org/stable/26292668.

Mateo-Lomba, P., Rivals, F., Blasco, R., Rosell, J., 2019. The use of bones as retouchers at Unit III of Teixoneres Cave (MIS 3; Moià, Barcelona, Spain). J. Archaeol. Sci. Rep. 27, 101980. https://doi.org/10.1016/j.jasrep.2019.101980.

McGrath, K., El-Zaatari, S., Guatelli-Steinberg, D., Stanton, M.A., Reid, D.J., Stoinski, T.S., Cranfield, M.R., Mudakikwa, A., McFarlin, S.C., 2018. Quantifying linear enamel hypoplasia in Virunga Mountain gorillas and other great apes. Am. J. Phys. Anthropol. 166 (2), 337-352. doi:10.1002/ajpa.23436.

Modesto-Mata, M., Dean, M.C., Bermúdez de Castro, J.M., Martinón-Torres, M., Rodríguez-Hidalgo, A., Marín, J., Canals, A., Vergès, J.M., Lozano, M., 2017. Perikymata numbers and enamel extension rates in the incisors of three archaeological modern human populations from two caves located in Spain: Maltravieso Cave (Cáceres) and Mirador Cave (Burgos). Quat. Int. 433, Part A, 114-123. http://dx.doi.org/10.1016/j.quaint.2015.07.024.

Ollé, A., Pedergnana, A., Fernández-Marchena, J. L., Martin, S., Borel, A., Aranda, V., 2016. Microwear features on vein quartz, rock crystal and quartzite: A study combining Optical Light and Scanning

Electron Microscopy. Quat. Int., 424 (Supplement C), 154-170. doi:https://doi.org/10.1016/j.quaint.2016.02.005

Pedergnana, A., Ollé, A., 2018. Building an Experimental Comparative Reference Collection for Lithic Micro-Residue Analysis Based on a Multi-Analytical Approach. J. Archaeol. Meth. Theor. 25 (1), 117-154. doi:10.1007/s10816-017-9337-z.

Power, R.C., Salazar-García, D.C., Straus, L.G., González Morales, M.R., Henry, A.G., 2015. Microremains from El Mirón Cave human dental calculus suggest a mixed plant–animal subsistence economy during the Magdalenian in Northern Iberia. J. Archaeol. Sci. 60(0):39-46. http://dx.doi.org/10.1016/j.jas.2015.04.003.

Robb, N.D., Cruwys, E., Smith, B.G.N., 1991. Regurgitation erosion as a possible cause of tooth wear in ancient British populations. Arch. Oral Biol. 36(8):595-602. https://doi.org/10.1016/0003-9969(91)90110-G.

Romero, A., De Juan, J., 2012. SEM, teeth, and palaeoanthropology: the secret of ancient human diets. In: Schatten H, (Ed.), Scanning Electron Microscopy for the Life Sciences. Cambridge: Cambridge University Press, pp. 236-256.

Ryan, A.S., Johanson, D.C., 1989. Anterior dental microwear in Australopithecus afarensis: comparisons with human and nonhuman primates. J. Hum. Evol. 18 (3), 235-268. doi:10.1016/0047-2484(89)90051-1.

Schmidt, C.W., Remy, A., Van Sessen, R., Willman, J., Krueger, K., Scott, R., Mahoney, P., Beach, J., McKinley, J., D'Anastasio, R., Chiu, L., Buzon, M., De Gregory, J.R., Sheridan, S., Eng, J., Watson, J., Klaus, H., Da-Gloria, P., Wilson, J., Stone, A., Sereno, P., Droke, J., Perash, R., Stojanowski, C., Herrmann, N., 2019. Dental microwear texture analysis of Homo sapiens sapiens: Foragers, farmers, and pastoralists. Am. J. Phys. Anthropol. 169 (2), 207-226. doi:10.1002/ajpa.23815.

Scott, G.R., Winn, J.R., 2011. Dental chipping: Contrasting patterns of microtrauma in Inuit and European populations. Int. J. Osteoarchaeol. 21 (6), 723-731. doi:10.1002/oa.1184.

Semprebon, G.M., Godfrey, L.R., Solounias, N., Sutherland, M.R., Jungers, W.L., 2004. Can low-magnification stereomicroscopy reveal diet? J. Hum. Evol. 47 (3), 115-144. doi:10.1016/j.jhevol.2004.06.004.

Sperduti, A., Giuliani, M.R., Guida, G., Petrone, P.P., Rossi, P.F., Vaccaro, S., Frayer, D.W., Bondioli, L., 2018. Tooth grooves, occlusal striations, dental calculus, and evidence for fiber processing in an Italian eneolithic/bronze age cemetery. Am. J. Phys. Anthropol. 167 (2), 234-243. doi:10.1002/ajpa.23619.

Tanga, C., Quintili, V., Tinarelli, R., D'Anastasio, R., Viciano, J., 2016. Non-masticatory dental lesions in the Samnite necropolis of Alfedena (V–III centuries BCE; central-southern Italy). J. Paleopathol. 26 (1), 15-26.

Teaford, M.F., 2007. Dental microwear and paleoanthropology: cautions and possibilities. In: Bailey, S.E., Hublin, J.-J., (Eds.), Dental Perspectives on Human Evolution: State of the Art Research in Dental Paleoanthropology. Dordrecht: Springer, pp. 345-368.

Teaford, M.F., Larsen, C.S., Pastor, R.F., Noble, V.E., 2001. Pits and scratches: microscopic evidence of tooth use and masticatory behavior in La Florida. In: Larsen, C.S. (Ed.), Bioarchaeology of Spanish Florida. Gainsville: University Press of Florida, pp. 82-112.

Tomczyk, J., Zalewska, M., 2016. Mechanical and chemical dental wear in historical population from the Syrian lower Euphrates valley. Arch. Oral Biol. 62, 49-57. http://dx.doi.org/10.1016/j.archoralbio.2015.11.011.

Turner, C.G., Machado, L.M.C., 1983. A new dental wear pattern and evidence for high carbohydrate consumption in a Brazilian archaic skeletal population. Am. J. Phys. Anthropol. 61, 125-130. https://doi.org/10.1002/ajpa.1330610113.

Ungar, P.S., 2019. Inference of Diets of Early Hominins from Primate Molar Form and Microwear. J. Dent. Res. 98 (4), 398-405. doi:10.1177/0022034518822981.

Ungar, P.S., Scott, R.S., Scott, J.R., Teaford, M., 2008. Dental microwear analysis: historical perspectives and new approaches. In: Irish, J.D., Nelson, G.C., (Eds.). Technique and application in dental anthropology. Cambridge: Cambridge University Press, pp. 389-425.

Vergès, J.M., Allué, E., Angelucci, D., Burjachs, F., Carrancho, A., Cebrià, A., Expósito, I., Fontanals, M., Moral, S., Rodríguez, A., 2008. Los niveles neolíticos de la cueva de El Mirador (Sierra de Atapuerca, Burgos): nuevos datos sobre la implantación y el desarrollo de la economía agropecuaria en la submeseta norte. In: Hernández-Pérez, M.S., Soler-Díaz, J.A., López-Padilla J.A., (Eds.), IV Congreso del Neolítico Peninsular. MARQ, Museo Arqueológico de Alicante: Diputación Provincial de Alicante, pp. 418-427.

Vergès, J.M., Allué, E., Angelucci, D.E., Cebrià, A., Díez, C., Fontanals, M., Manyanós, A., Montero, S., Moral, S., Vaquero, M., 2002. La Sierra de Atapuerca durante el Holoceno: datos preliminares sobre las ocupaciones de la Edad del Bronce en la cueva de El Mirador (Ibeas de Juarros, Burgos). Trab. Prehist. 59 (1), 107-126. https://doi.org/10.3989/tp.2002.v59.i1.213.

Vergès, J.M., Allué, E., Fontanals, M., Morales, J.I., Martín, P., Carrancho, Á., Expósito, I., Guardiola, M., Lozano, M., Marsal, R., 2016. El Mirador cave (Sierra de Atapuerca, Burgos, Spain): A whole perspective. Quat. Int. 414, 236-243. https://doi.org/10.1016/j.quaint.2016.01.044.

Vergès, J.M., Morales, J.I., 2014. The gigapixel image concept for graphic SEM documentation. Applications in archeological use-wear studies. Micron. 65, 15-19. http://dx.doi.org/10.1016/j.micron.2014.04.009.

Willman, J.C., 2016. Dental wear at Dolní Věstonice II: Habitual behaviors and social identities written on teeth. In: Svoboda. J., (Ed.), Dolní Věstonice II: Chronostratigraphy, Paleoethnology, Paleoanthropology. Brno: Archeologický ústav AV ČR, pp. 353-371.

Willman, J.C., 2017. The dental remains: non-masticatory wear In: Trinkaus, E., Walker, M.J., (Eds.), The People of Palomas: Neandertals from the Sima de las Palomas, Cabezo Gordo, Southeastern Spain. College Station: Texas A&M University Press, pp. 155-174.

Willman, J.C., Ginter, B., Hernando, R., Lozano, M., Sobczyk, K., Stefański, D., Szczepanek, A., Wertz, K., Wojtal, P., Zając, M., Zarzecka-Szubińska, K., Valde-Nowak, P., 2019. Paleobiology and Taphonomy of a Middle Paleolithic Neandertal Tooth from Ciemna Cave, Southern Poland. J. Paleol. Archaeol. 2 (4), 359-377. doi:10.1007/s41982-019-00026-4.

Willman, J.C., Hernando, R., Matu, M., Crevecoeur, I. 2020. Biocultural diversity in Late Pleistocene/Early Holocene Africa: Olduvai Hominid 1 (Tanzania) biological affinity and intentional body modification. Am. J. Phys. Anthropol. 1-18. doi:10.1002/ajpa.24007.

Willoughby, P.R., Compton, T., Bello, S.M., Bushozi, P.M., Skinner, A.R., Stringer, C.B., 2018. Middle Stone Age human teeth from Magubike rockshelter, Iringa Region, Tanzania. PLOS ONE 13 (7), e0200530. doi:10.1371/journal.pone.0200530.

Xing, S., O'Hara, M., Guatelli-Steinberg, D., Ge, J., Liu, W., 2017. Dental scratches and handedness in East Asian Early Pleistocene hominins. Int. J. Osteoarchaeol. 27 (6), 937-946. doi:10.1002/oa.2601.

FIGURE CAPTIONS

Figure 1. Gigapixel-like (GPL) image of the labial surface of ATA09-MIR201-REM-489, a left I_2, from El Mirador Cave with 1 mm scale (center) and call-out boxes features surfaces details under various magnifications. Number next to each call-out box indicates the magnification used relative to the complete GPL image. Descriptions proceed clockwise from upper right corner. *Orange rectangle*: Medium size antemortem enamel chip with well-worn margins. *Green rectangle*: Detail of cementoenamel junction and root surface. Subtle perikymata (bottom left quadrant) and striations (upper left quadrant) are visible on the enamel. Subtle postmortem cracking of root surface also evident. *Magenta rectangle*: Detail of furrow-form hypoplasia with clearly visible perikymata (between white arrows). Black arrow points to dental calculus deposit. *White rectangle*: Detail of instrumental striation with a right oblique orientation. *Blue rectangle*: arrows indicate microstriations on labio-incisal edge and a well-worn, but small, antemortem enamel chip to the left of the image.

Figure 2. Gigapixel-like (GPL) image of the lingual surface of ATA12-MIR201-S36-69, a right I^1, from El Mirador Cave with 1 mm scale (center) and call-out boxes features surfaces details under various magnifications. Number next to each call-out box indicates the magnification used relative to the complete GPL image. Descriptions proceed clockwise from upper right corner. *Orange rectangle*: Detail of the margin of a faint continuous cingular lesion (CCL). Cementoenamel junction and root surface also visible. *Green rectangle*: Detail of a medium-sized antemortem enamel chip with well-rounded edges. Occlusal edge exhibits some pitting and microstriations. *Magenta rectangle*: Detail of occlusal surface showing postdepositional cracking of dentin and enamel. *White rectangle*: Detail of portion of lingual fossa showing well-worn surface and exogenous materials in deepest recesses. *Blue rectangle*: Detail of faint CCL. *Yellow arrows*: dentin exposure characteristic of lingual surface attrition of the maxillary anterior teeth (LSAMAT).

Figure 3. Macrophotograph with call-out (black box) for gigapixel-like (GPL) image of a portion of the labial surface of ATA-MIR201-S36-68, a right I^1, from El Mirador Cave. Scales are 1 mm. Call-out boxes with dashed borders represent 4x magnification relative to the central GPL image. Note the broad area of dull and darkened enamel in the middle third of the macrophotograph. Descriptions proceed clockwise from upper left corner. *Blue rectangle*: Detail of enamel near cervix. Large inclusion is a calculus deposit. Note a lack of striations, visible perikymata, and small flecks of calculus. *Orange rectangle*: Heavily striated surface. Striations are predominately horizontal or low-oblique angles. *Green rectangle*: Heavily striated surface. Striations are predominately horizontal or low-oblique angles. Many of the striations are wider and deeper with well-worn edges compared to example above (orange rectangle). *Magenta rectangle*: Appearance very similar to example above (green rectangle).

Figure 4. Gigapixel-like (GPL) image of a portion of the labial surface of ATA-MIR201-S36-68, a right I^1, from El Mirador Cave with 1 mm scale bar. Orange dashed call-out box shows area examined at 300x magnification (with 300 μm scale bar). The solid-border call-out box indicates the area of the micrograph that is magnified 3x in the bottom image to show the characteristic “honeycomb” pattern of enamel prism erosion as well as some horizontal striations. These images were not used for the creation of the GPL image.

Figure Captions

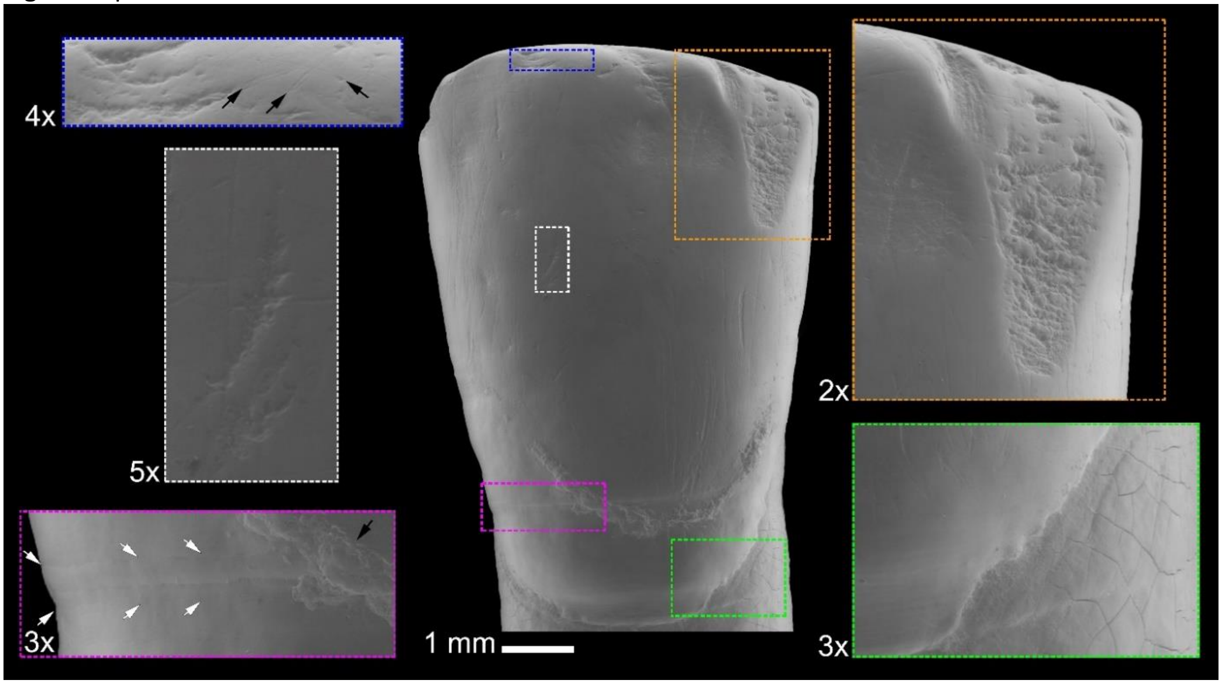

Figure 1. Gigapixel-like (GPL) image of the labial surface of ATA09-MIR201-REM-489, a left I_2, from El Mirador Cave with 1 mm scale (center) and call-out boxes features surfaces details under various magnifications. Number next to each call-out box indicates the magnification used relative to the complete GPL image. Descriptions proceed clockwise from upper right corner. *Orange rectangle*: Medium size antemortem enamel chip with well-worn margins. *Green rectangle*: Detail of cementoenamel junction and root surface. Subtle perikymata (bottom left quadrant) and striations (upper left quadrant) are visible on the enamel. Subtle postmortem cracking of root surface also evident. *Magenta rectangle*: Detail of furrow-form hypoplasia with clearly visible perikymata (between white arrows). Black arrow points to dental calculus deposit. *White rectangle*: Detail of instrumental striation with a right oblique orientation. *Blue rectangle*: arrows indicate microstriations on labio-incisal edge and a well-worn, but small, antemortem enamel chip to the left of the image.

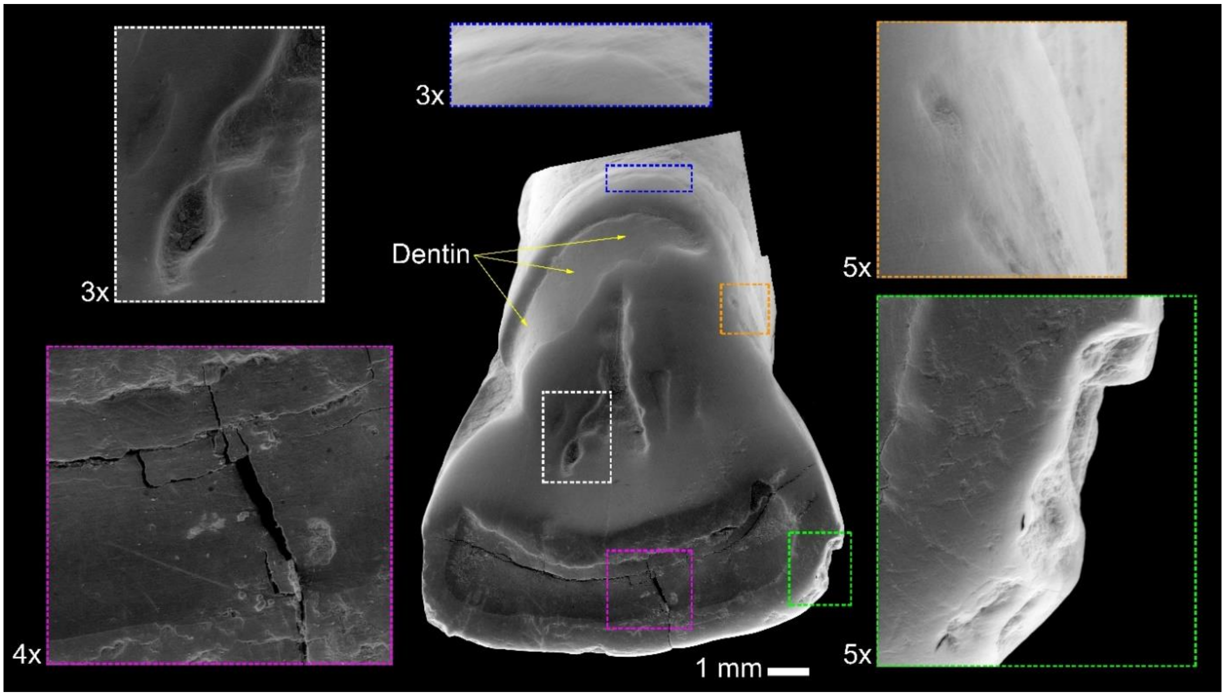

Figure 2. Gigapixel-like (GPL) image of the lingual surface of ATA12-MIR201-S36-69, a right I^1, from El Mirador Cave with 1 mm scale (center) and call-out boxes features surfaces details under various magnifications. Number next to each call-out box indicates the magnification used relative to the complete GPL image. Descriptions proceed clockwise from upper right corner. *Orange rectangle*: Detail of the margin of a faint continuous cingular lesion (CCL). Cementoenamel junction and root surface also visible. *Green rectangle*: Detail of a medium-sized antemortem enamel chip with well-rounded edges. Occlusal edge exhibits some pitting and microstriations. *Magenta rectangle*: Detail of occlusal surface showing postdepositional cracking of dentin and enamel. *White rectangle*: Detail of portion of lingual fossa showing well-worn surface and exogenous materials in deepest recesses. *Blue rectangle*: Detail of faint CCL. *Yellow arrows*: dentin exposure characteristic of lingual surface attrition of the maxillary anterior teeth (LSAMAT).

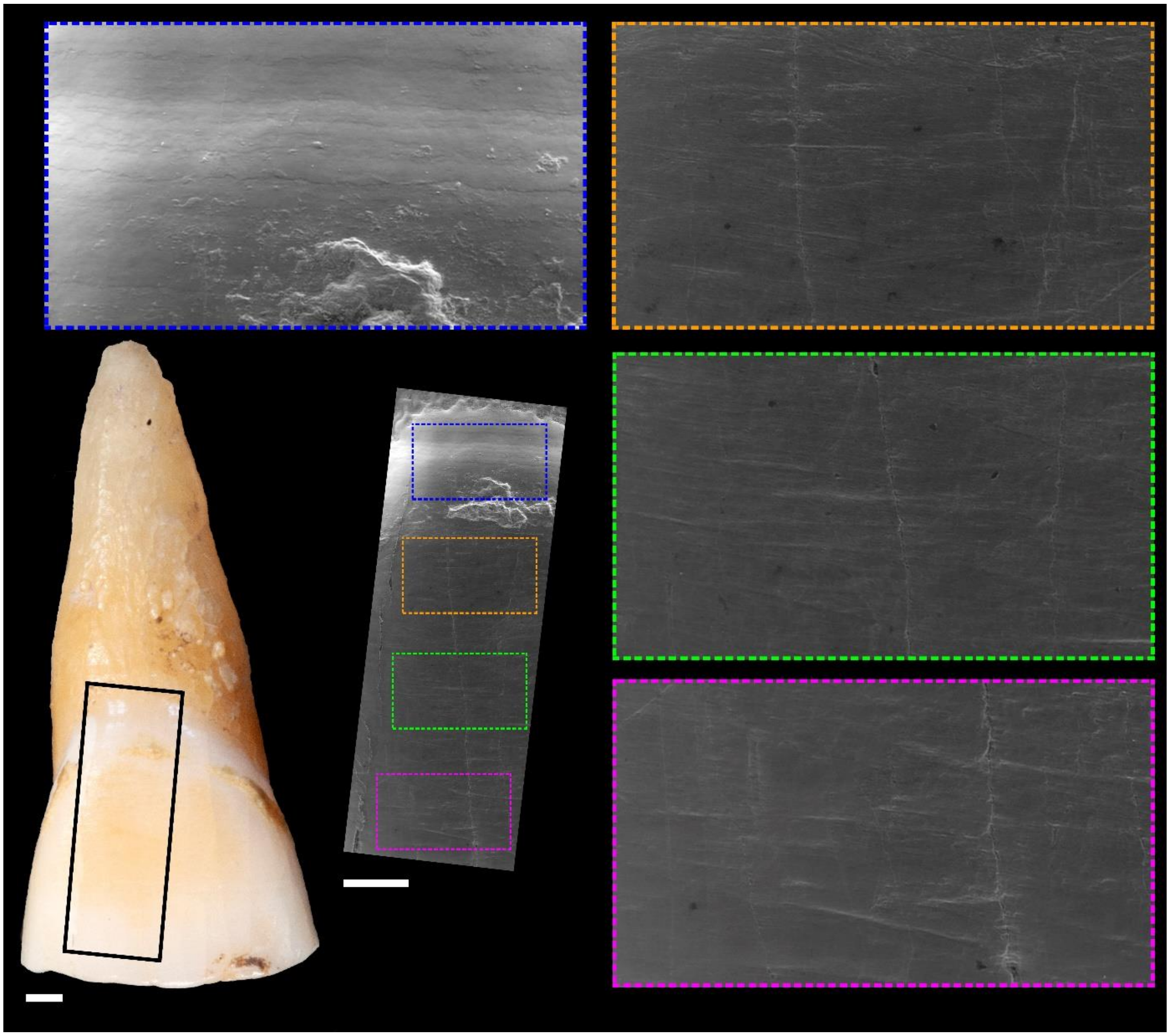

Figure 3. Macrophotograph with call-out (black box) for gigapixel-like (GPL) image of a portion of the labial surface of ATA-MIR201-S36-68, a right I^1, from El Mirador Cave. Scales are 1 mm. Call-out boxes with dashed borders represent 4x magnification relative to the central GPL image. Note the broad area of dull and darkened enamel in the middle third of the macrophotograph. Descriptions proceed clockwise from upper left corner. *Blue rectangle*: Detail of enamel near cervix. Large inclusion is a calculus deposit. Note a lack of striations, visible perikymata, and small flecks of calculus. *Orange rectangle*: Heavily striated surface. Striations are predominately horizontal or low-oblique angles. *Green rectangle*: Heavily striated surface. Striations are predominately horizontal or low-oblique angles. Many of the striations are wider and deeper with well-worn edges compared to example above (orange rectangle). *Magenta rectangle*: Appearance very similar to example above (green rectangle).

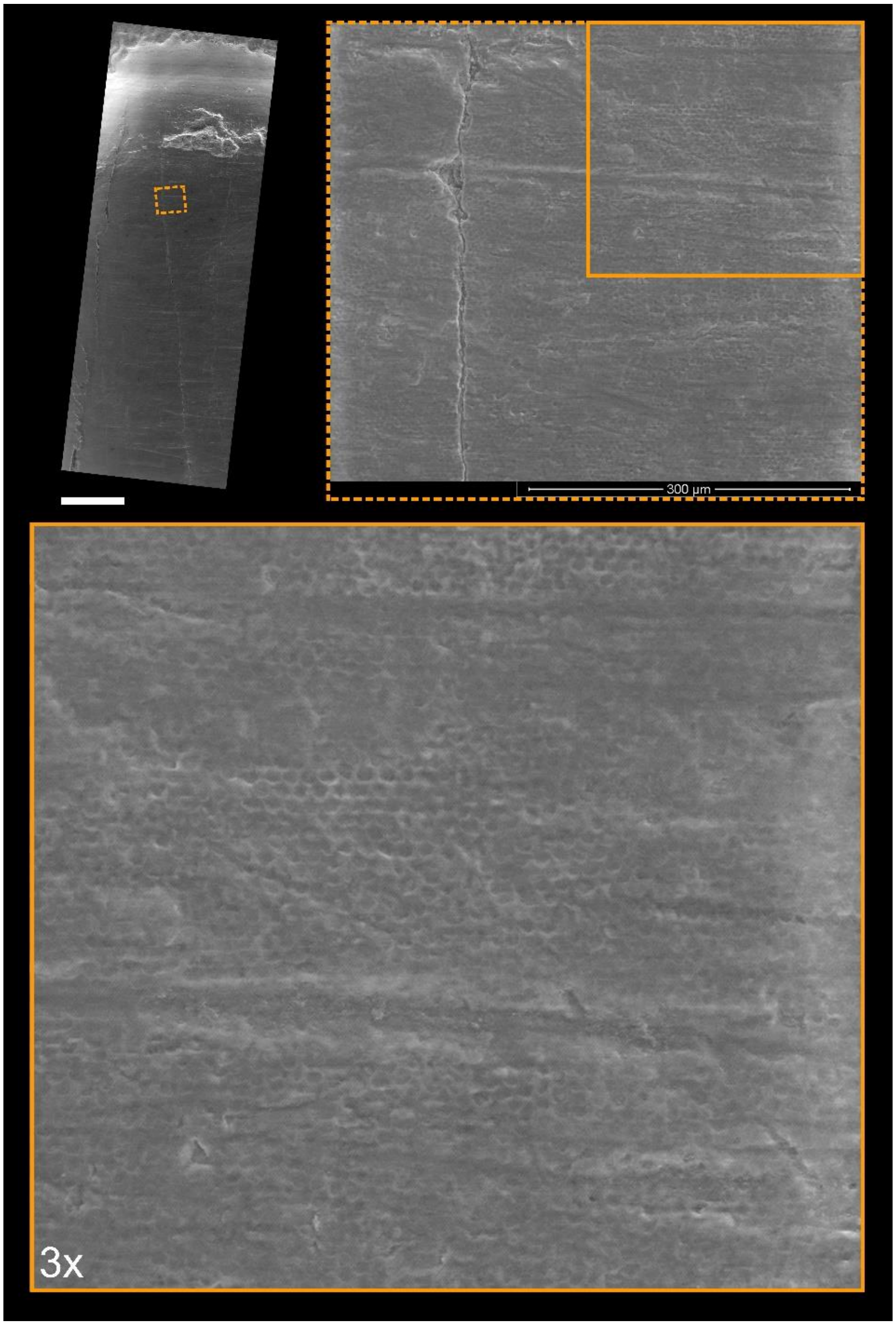

Figure 4. Gigapixel-like (GPL) image of a portion of the labial surface of ATA-MIR201-S36-68, a right I^1, from El Mirador Cave with 1 mm scale bar. Orange dashed call-out box shows area examined at 300x magnification (with 300 µm scale bar). The solid-border call-out box indicates the area of the micrograph that is magnified 3x in the bottom image to show the characteristic “honeycomb” pattern of enamel prism erosion as well as some horizontal striations. These images were not used for the creation of the GPL image.